

# Novel screening techniques for ion channel targeting drugs

Alison Obergrussberger<sup>1</sup>, Sonja Stölzle-Feix<sup>1</sup>, Nadine Becker<sup>1</sup>, Andrea Brüggemann<sup>1</sup>, Niels Fertig<sup>1,\*</sup>, and Clemens Möller<sup>2,\*</sup>

<sup>1</sup>Nanion Technologies GmbH; Munich, Germany; <sup>2</sup>Albstadt-Sigmaringen University; Life Sciences Faculty; Sigmaringen, Germany

**Keywords:** Automated patch clamp, action potential, cardiomyocytes, Electrophysiology, ion channels, impedance, screening, safety pharmacology, temperature

Ion channels are integral membrane proteins that regulate the flux of ions across the cell membrane. They are involved in nearly all physiological processes, and malfunction of ion channels has been linked to many diseases. Until recently, high-throughput screening of ion channels was limited to indirect, e.g. fluorescence-based, readout technologies. In the past years, direct label-free biophysical readout technologies by means of electrophysiology have been developed. Planar patch-clamp electrophysiology provides a direct functional label-free readout of ion channel function in medium to high throughput. Further electrophysiology features, including temperature control and higher-throughput instruments, are continually being developed. Electrophysiological screening in a 384-well format has recently become possible. Advances in chip and microfluidic design, as well as in cell preparation and handling, have allowed challenging cell types to be studied by automated patch clamp. Assays measuring action potentials in stem cell-derived cardiomyocytes, relevant for cardiac safety screening, and neuronal cells, as well as a large number of different ion channels, including fast ligand-gated ion channels, have successfully been established by automated patch clamp. Impedance and multi-electrode array measurements are particularly suitable for studying cardiomyocytes and neuronal cells within their physiological network, and to address more complex physiological questions. This article discusses recent advances in electrophysiological technologies available for screening ion channel function and regulation.

## Introduction

Each cell is separated from its environment by a lipid membrane. Ion channels embedded in the membrane regulate the flux

of ions across the cell membrane. They are involved in nearly all physiological processes, and malfunction of ion channels has been linked to many diseases. Therefore, ion channels have been extensively studied as drug targets, and owing to their potential role in drug discovery they have been termed the “next GPCRs.”<sup>1</sup> In addition, ion channels are responsible for a number of drug side effects, most prominently cardiac arrhythmia, potentially induced by effects of drugs on cardiac ion channels, in particular the hERG ion channel. The importance of investigating these side effects is emphasized by regulatory guidelines and documents currently in development.<sup>2</sup> High-throughput screening assays for ion channels have been established in pharmaceutical companies using indirect readout technologies, often with fluorescent assays, e.g., by monitoring the change of the cellular potential with potentiometric dyes, or by fluorescence-labeling known ligands.<sup>3</sup> These methods provide an indirect measure of ion channel function. In addition, over the past years direct label-free biophysical technologies for screening ion channels by means of electrophysiology have been developed. These enable functional high throughput screening of ion channels and provide insight into function and regulation of ion channels, even within their cellular environment.

## The Patch Clamp Technique

The patch clamp technique first described in the 1970s by Neher and Sakmann<sup>4</sup> remains the gold standard for studying ion channel function. The technique involves bringing a fine glass pipette in close contact with the cell membrane under the control of a skilled operator using a microscope and fine micromanipulator. A tight seal, in the GΩ range, is then formed between the glass of the pipette and the cell membrane. Once a tight seal is formed, the small patch of membrane which plugs the end of the pipette can be ruptured, forming a continuous electrical circuit between the internal solution and electrode contained within the patch clamp pipette, and the inside of the cell, a configuration known as the whole cell patch clamp technique (Fig. 1A). In this way, openings and closings of ion channels can be monitored in terms of electrical current. The ion channel activity which occurs over the whole of the cell membrane is measured in response to external stimuli, typically either voltage or ligand, but also temperature or mechanical stress. The technique

© Alison Obergrussberger, Sonja Stölzle-Feix, Nadine Becker, Andrea Brüggemann, Niels Fertig, and Clemens Möller

\*Correspondence to: Clemens Möller; Email: Clemens.Moeller@hs-albsig.de; Niels Fertig; Email: Niels.Fertig@nanion.de

Submitted: 07/29/2015; Accepted: 07/30/2015

<http://dx.doi.org/10.1080/19336950.2015.1079675>

This is an Open Access article distributed under the terms of the Creative Commons Attribution-Non-Commercial License (<http://creativecommons.org/licenses/by-nc/3.0/>), which permits unrestricted non-commercial use, distribution, and reproduction in any medium, provided the original work is properly cited. The moral rights of the named author(s) have been asserted.

yields data which is extremely information rich but is notoriously low throughput and requires skilled personnel with years of training to perform the experiments. As well as a microscope and micromanipulator, other pieces of equipment to minimise electrical interference and vibration, in the form of a Faraday cage and anti-vibration table, respectively, are also essential parts of a conventional patch clamp rig.

### Automation of the Patch Clamp Technique

Soon after the introduction of the patch clamp technique, the race to automate the technique began. The goal of automation was to improve ease of use and increase throughput by parallelization. One of the most successful methods for automation involves replacing the patch clamp pipette with a planar glass chip perforated with one (or, recently, a number of) aperture

(Fig. 1B). The first successful recordings of cells and bilayers on a planar glass chip were described in 2002.<sup>5</sup> In these initial recordings, quartz glass was used for the glass substrate because of its dielectric properties. Nowadays, in common with the majority of conventional patch clamp experiments, borosilicate glass is used for its low capacitance, and, therefore, low noise. A cell is attracted to the patch clamp aperture of the glass chip by the use of suction from underneath. Following this, a tight seal is formed between the glass chip and the cell membrane in the same way as in the conventional patch clamp technique. Similarly, the cell membrane is ruptured and electrical access gained to the inside of the cell. The planar design and the use of suction negate the need for a microscope, micromanipulator and anti-vibration table, making these devices smaller and more compact. Incorporating the glass chip into a robotic environment provides a means to fully automate and parallelize the experiments to increase throughput.

To date, a number of planar patch clamp systems have been developed, ranging from small devices recording from a single cell at a time, e.g. the Port-a-Patch (Nanion Technologies), through medium throughput devices, e.g., the Patchliner (Nanion Technologies), PatchXpress (Molecular Devices) and QPatch (Sophion A/S), up to high throughput devices such as the SyncroPatch 96 (Nanion Technologies), IonFlux (Fluxion), Qube (Sophion A/S), IonWorks Barracuda (Molecular Devices) and, most recently, the SyncroPatch 384PE (Nanion Technologies). These devices differ in their flexibility, diversity of experimental protocols, quality of data and throughput. Table 1 provides a comparison of available automated patch clamp systems. The first part of this review focuses on recent advances on the devices Port-a-Patch, Patchliner and SyncroPatch 384PE from Nanion Technologies. For a more comprehensive review of available systems, please see Dunlop et al. and Bebarova.<sup>6,7</sup>

In the case of semi-automated devices such as the Port-a-Patch, operation offers a similar experimental flexibility to conventional patch clamp, with the added advantage of easy exchange of the internal solution<sup>8</sup> so that actions of compounds on the inside of the cell membrane can be investigated with relative ease. The Port-a-Patch is used in academia and industry alike for basic ion channel research and drug discovery. Cell lines such as HEK and CHO cells are used with equal success rates and experiments can be performed at room or physiological temperature.<sup>8</sup> Additionally, primary cells such as human corneal epithelial cells,<sup>9</sup> stem cell-derived cardiomyocytes<sup>10</sup> and lysosomes<sup>11</sup>

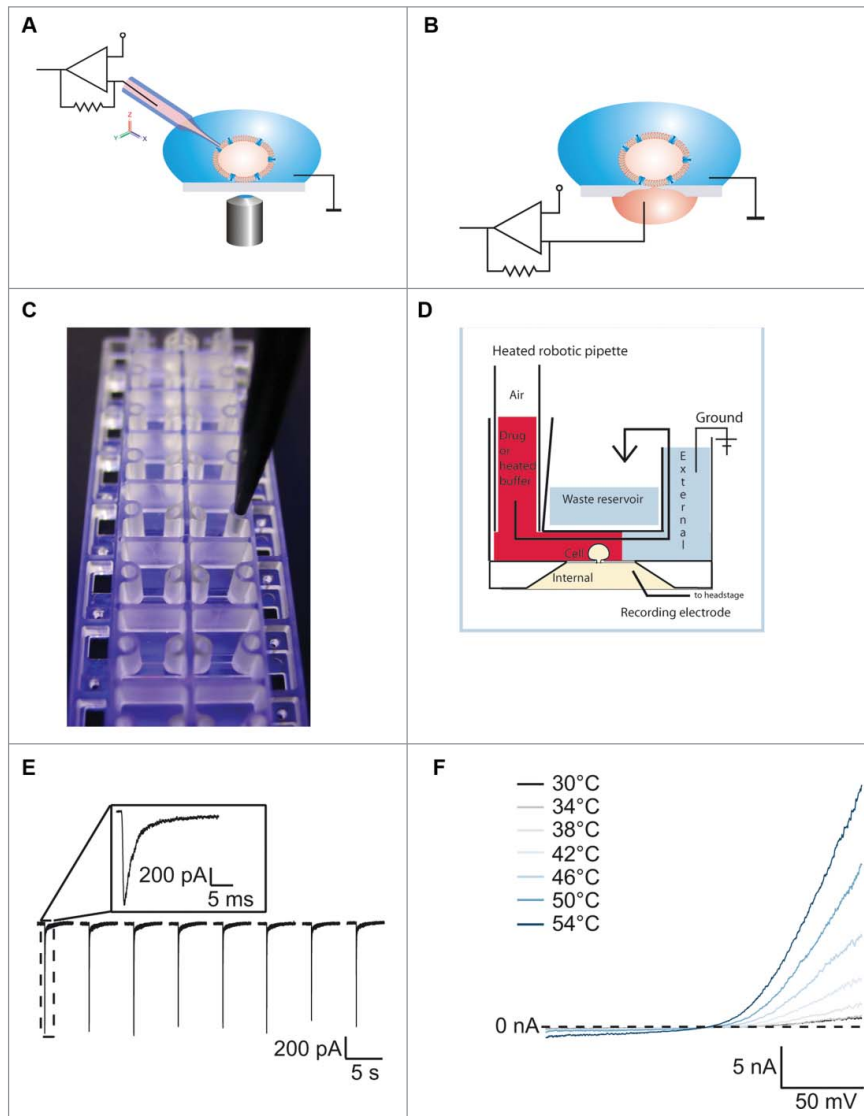


Figure 1. For figure legend, see next page.

have been used successfully. As the data recorded is low noise and high resolution, single channel recordings in the cell attached mode on the cell membrane, and experiments recording ion channels reconstituted into lipid bilayers, are also routinely performed using the Port-a-Patch.<sup>12</sup> Recently, the flexibility of the Port-a-Patch has been further emphasized by its application to measuring the translocation of antibiotic drugs through single porins reconstituted into bilayers, thereby paving the way to studying one mechanism of bacterial antibiotic resistance.<sup>13</sup>

## Flexibility and Throughput

In order to increase throughput, robotic systems have been introduced which record from multiple cells in parallel. This can be done using a chip with a single hole per well such as the Patchliner, SyncroPatch 96, SyncroPatch 384PE, PatchXpress and QPatch, or multiple holes per well as in the IonWorks Quattro and IonWorks Barracuda. The Patchliner is a fully automated planar patch clamp robotic system recording from up to 8 cells simultaneously. Its medium throughput properties are complemented with useful features such as internal solution exchange, temperature control and current clamp.<sup>14</sup> The chip design is such that micro-fluidic channels are formed (Fig. 1C, D). The exchange time is fast (< 10 ms) and compound volume requirements are low (< 25  $\mu$ l per well to completely exchange the solution). Additionally, solutions can be stacked inside the pipette of the Patchliner to minimise compound exposure time.<sup>8</sup> In this way, challenging ligand-gated ion channel targets such as the nicotinic acetylcholine  $\alpha$ 7 receptor (nACh $\alpha$ 7R) can be reliably and reproducibly recorded on the Patchliner (Fig. 1E), and on the QPatch.<sup>15–17</sup> The temperature control feature on instruments such as Patchliner and Ionflux<sup>18</sup> can be used to record ion channel activity at physiological temperature, and on the Patchliner, fast changes in temperature can be used to activate temperature regulated ion channels such as TRPV1<sup>19</sup> and TRPV3<sup>14</sup> (Fig. 1F). A number of cell lines including HEK293, CHO, LTK, RBL, SHSY5Y, GH4C1, ND7–23 and jurkat are routinely

used on the Patchliner with equally high success rates. In addition, currents from primary cells such as rat cortical astrocytes,<sup>20</sup> human fibroblast-like synoviocytes,<sup>20</sup> red blood cells<sup>21</sup> and vascular smooth muscle cells<sup>22</sup> have been successfully recorded.

Cardiomyocytes derived from pluripotent stem cells (iPS) are receiving increasing attention as a potential model for safety screening and toxicology for early screening of lead compounds.<sup>23,24</sup> Recently the Food and Drug Administration (FDA) and the Health and Environmental Sciences Institute (HESI) started a new initiative to evaluate the potential for integrated non-clinical cardiac ion channel activity assessment to predict the clinical pro-arrhythmic risk of drugs.<sup>2,25</sup> Included in this is the evaluation of the use of pluripotent stem cell applications for cardiovascular risk assessment. So far, the Patchliner has been used successfully to record from mouse embryonic stem cells (CorAt, Axiogenesis),<sup>10</sup> human iPS cells from CDI,<sup>14,26</sup> Axiogenesis (Cor.4U)<sup>26</sup>, and Collectis (Fig. 2A, B). Importantly, individual ion channel currents relevant for safety testing such as Na<sub>v</sub>1.5 can be recorded in the voltage clamp mode, and the effect of compounds on the action potential in the current clamp mode can be measured. Figure 2A shows the current-voltage plot of an average of 4 iPS cardiac cells (Collectis) and the current responses to increasing voltage in the voltage clamp mode of an exemplar cell recorded on the Patchliner. The currents recorded are characteristic of a voltage-gated Na<sup>+</sup> channel. Additionally, Figure 2B shows block of the current in the voltage clamp mode by tetracaine and the effect of tetracaine on the action potentials elicited in the same cell. Assays for cardiac safety evaluations are also developed on other automated patch clamp devices, and are increasingly combined with additional assays improving an integrated cardiac risk assessment.<sup>27</sup>

Stem cell-derived neurons could provide important models for diseases such as Alzheimer. Recently, iPS neurons (CDI) have been used successfully in both conventional electrophysiology and on the Patchliner.<sup>26,28</sup> In these cells, a voltage-gated Na<sup>+</sup> channel, K<sup>+</sup> channel and the ligand-gated ion channel, the GABA<sub>A</sub> receptor, could be recorded (Fig. 2C, D). Additionally, action potentials could be generated in some cells (Fig. 2E).

**Figure 1 (See previous page).** (A) Schematic of conventional patch clamp set-up showing the patch clamp pipette attached to the cell membrane. The cell is attached to the bottom of the dish and is viewed using a microscope. A ground electrode is positioned in the external solution and the internal electrode in the patch clamp pipette is attached to the amplifier headstage. Reproduced with permission from Brüggemann et al.<sup>42</sup> © Wiley. Reproduced by permission of Bettina Loycke. Permission to reuse must be obtained from the rightsholder. (B) Schematic of a planar patch clamp set-up as used for the Port-a-Patch, Patchliner, SyncroPatch 96 and SyncroPatch 384PE. Here the cell is attached to the glass of the patch clamp chip. A ground electrode is positioned in the external solution and the internal electrode at the bottom of the planar chip is attached to the amplifier headstage. Reproduced with permission from Brüggemann et al.<sup>42</sup> © Wiley. Reproduced by permission of Bettina Loycke. Permission to reuse must be obtained from the rightsholder. (C) The Patchliner chip. The planar glass layer which contains the patch clamp aperture is sandwiched between 2 plastic molds creating micro-fluidic channels. The pipette of the Patchliner is shown positioned in the channel for delivering external solution, cells and compounds. (D) Schematic of the Patchliner chip. The cell is shown positioned on the patch clamp aperture in the whole cell configuration. When solutions are added on the external side, the existing solution is pushed into the waste chamber and the external solution is completely exchanged. The waste chamber is emptied continuously using an external waste pump. (E) The Patchliner was used to repetitively activate nACh $\alpha$ 7R expressed in HEK cells by nicotine on the Patchliner. The solutions were stacked inside the pipette of the Patchliner to minimise exposure time. Shown are 8 consecutive applications of 100  $\mu$ M nicotine. Peak amplitude is consistent over all 8 applications. Inset shows nACh $\alpha$ 7R activation of the first application expanded. Reproduced with permission from Obergrussberger et al.<sup>17</sup> © Wiley. Reproduced by permission of Paulette Goldweb. Permission to reuse must be obtained from the rightsholder. (F) Current traces of TRPV3 expressed in HEK cells when activated by heated solution. External solution was heated inside the pipette of the Patchliner to the temperature shown and applied to the cell. Currents started to activate at  $\geq 38^\circ\text{C}$ . (Reproduced with permission from Stoelzle et al.<sup>14</sup> © Sonja Stoelzle-Feix, reproduced by permission of Sonja Stoelzle-Feix. Permission to reuse must be obtained from the rightsholder.

**Table 1.** Comparison of automated patch clamp devices available on the market. Information contained within the table was collected from relevant company websites: [www.nanion.de](http://www.nanion.de); [www.moleculardevices.com](http://www.moleculardevices.com); [www.sophion.com](http://www.sophion.com) and [www.fluxionbio.com](http://www.fluxionbio.com). \* 16 amplifier channels and a multiplexer are used. \*\* 10 ms for Fast Perfusion Kit for the Port-a-Patch and 100 ms for standard External Perfusion System. \*\*\* rough estimates from the manufacturers and vendors, depending on cells, protocols etc.

Instrument	Port-a-Patch	Patchliner	PatchXpress	QPatch	SynroPatch 96	IonFlux	Qube	IonWorks Barracuda	SynroPatch 384PE
Company	Nanion	Nanion	MDS	Biolin Scientific (Sophion)	Nanion	Fluxion	Biolin Scientific (Sophion)	MDS	Nanion
Recording substrate	Glass, single hole or multiple holes per well	Glass, single hole or multiple holes per well	Glass, single hole per well	Silicon, single hole or multiple holes per well	Glass, single hole or multiple holes per well	PDMS, Single hole or 20 holes per well	Polymer, single hole or 10 holes per well	Polymer, single hole or population patch with 64 holes per well	Glass, single hole or multiple holes per well
Recording configurations	Whole cell, cell attached, perforated patch, bilayer recordings.	Whole cell, cell attached, perforated patch, bilayer recordings.	Whole cell	Whole cell	Whole cell, perforated patch	Whole cell	Whole cell	Perforated patch (loose patch)	Whole cell, perforated patch
No. parallel recordings	1	4 or 8	16	8, 16 or 48	96*	16 or 64	384	384	384/768
Throughput***	50 data points/day	250-500 data points/day	500 compounds per 8 hour day	250-3000 data points/day	6000 data points/day	2500-8000 data points/day	30,000 compounds per 24 hours	1100 - 6000 data points/hour	20,000-38,000 data points/day
Seal resistance	GΩ	GΩ	GΩ	GΩ	GΩ	GΩ	GΩ	50-100 MΩ	GΩ
Compatible cells	Cell lines, primary cells, stem cells	Cell lines, primary cells, stem cells	Cell lines, stem cells	Cell lines, stem cells	Cell lines, stem cells	Cell lines, primary cells	Cell lines	Cell lines	Cell lines, stem cells
Temperature control	Optional	Optional	No	Optional	No	Yes (up to 40°C)	Not known	No	Optional
Current clamp	Yes	Yes	Yes	Yes	No	No	Not known	No	Yes
Number of pipettes	N/A	1	16	2, 4 or 8	16	N/A	384	384	384
External solution exchange time	10 - 100 ms**	10 ms	10-15 ms	10 ms	100 ms	100 ms	Not known	40 ms (single hole per well) to 80 ms (Population patch)	50 ms
Internal solution exchange	Yes	Yes	No	No	Yes	No	No	No	Yes

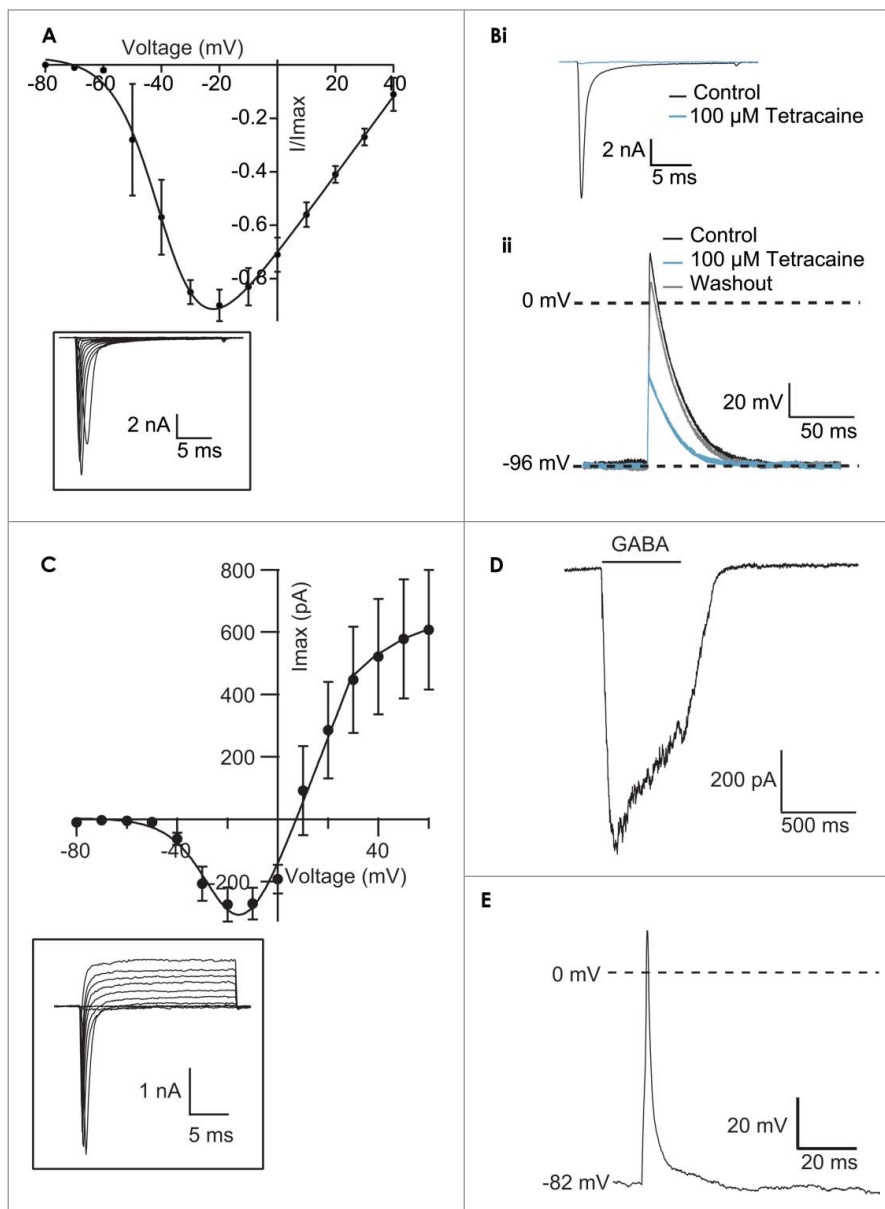


**Figure 2.** (A) Current-voltage plot of an average of 4 iPS cardiac cells (Cellctis) recorded on one run of the Patchliner. The currents were normalized to the maximum peak amplitude. The inset shows raw traces from an exemplar cell in response to voltage steps from  $-80$  mV to  $40$  mV. Currents started to activate about  $-50$  mV and peak response was elicited at around  $-20$  mV. **Bi** Current responses of an iPS cardiac cell to a voltage protocol to  $-20$  mV from a holding potential of  $-120$  mV in control conditions and in the presence of  $100 \mu\text{M}$  tetracaine. Tetracaine almost completely blocked the current response at this concentration, an effect that was completely reversible upon washout (trace not shown). **Bii** Action potentials were elicited in the current clamp mode using a  $1$  ms depolarizing current pulse. A holding current of  $-185$  pA was used to maintain a baseline voltage of  $-96$  mV. The action potential in control conditions is shown in black. The sodium channel blocker, tetracaine, at  $100 \mu\text{M}$  was applied and this inhibited the action potentials (blue). The effect could be reversed upon washout (gray). **(C)** Current-voltage relationship of an average of 54 iPS neurons (CDI) recorded on the Patchliner. The inset shows raw traces from an exemplary cell showing  $\text{Na}_v$  and  $\text{K}_v$  currents present in the cell. Fast, transient inward  $\text{Na}_v$  currents started to activate at about  $-40$  mV, and peak currents were elicited at  $-10$  mV or  $-20$  mV. **(D)** Activation of currents in iPS neurons (CDI) by the ligand GABA ( $30 \mu\text{M}$ ). GABA was applied for approximately  $600$  ms before washout with external solution using a stacked solutions approach. Cells were held at a constant holding potential of  $-70$  mV. **(E)** Action potential elicited from an iPS neuron (CDI) recorded on the Patchliner. Action potentials were elicited using a  $2$ ms depolarizing pulse. Panels (C-E) reproduced with permission from Haythornthwaite et al.<sup>28</sup> © SAGE. Reproduced by permission of Michelle Binur. Permission to reuse must be obtained from the rightsholder.

## High throughput and High Fidelity

The further development of automated patch clamp devices is ongoing. For high-throughput screening efforts, indirect read-out technologies such as fluorescence assays are still used, and combined with electrophysiological patch clamp compound characterization at later stages of compound development.<sup>29,30</sup> The demand for increasing throughput in electrophysiological screening, while maintaining high resolution data acquisition, however, calls for the introduction of new patch clamp devices with higher throughput. The SyncroPatch 384PE is an example of such a device. The chip of the SyncroPatch 384PE is a 384 well micro-titer-plate format with a borosilicate glass bottom. In each well is a single patch clamp aperture. A 384 channel amplifier guarantees that all cells are continuously voltage clamped during the recordings and this, coupled with a 384-pipettor head, ensures that all 384 cells are recorded truly in parallel. This results in an immense increase in throughput, in the order of 20,000 data points per day. Ease of use and powerful data handling software are paramount to the success of such a high throughput device. The data acquisition and analysis software for the SyncroPatch 384PE provides a color-coded, user-friendly interface where the user gains an impression of the success of the experiment at a glance. A screenshot of the software during an experiment recording simultaneously 6 different cardiac channels in 6 separate cells lines is shown in **Figure 3**. In this experiment, CHO cells expressing either  $\text{Cav}1.2$ ,  $\text{Nav}1.5$ ,  $\text{Kv}4.3$  or  $\text{Kv}7.1$ , or HEK cells expressing hERG or Kir2.1 (all cell lines provided by ChanTest, a Charles River Company) were captured to the patch clamp chip. Four columns of the patch clamp chip received the same cell line giving  $n = 64$  for each cell line. A specially designed voltage protocol (shown at the top of **Fig. 3**) was used to activate all voltage-gated currents simultaneously.

## Impedance Measurements and Multi-Electrode Arrays

As noted above, the patch clamp technique is widely used to measure ion channel

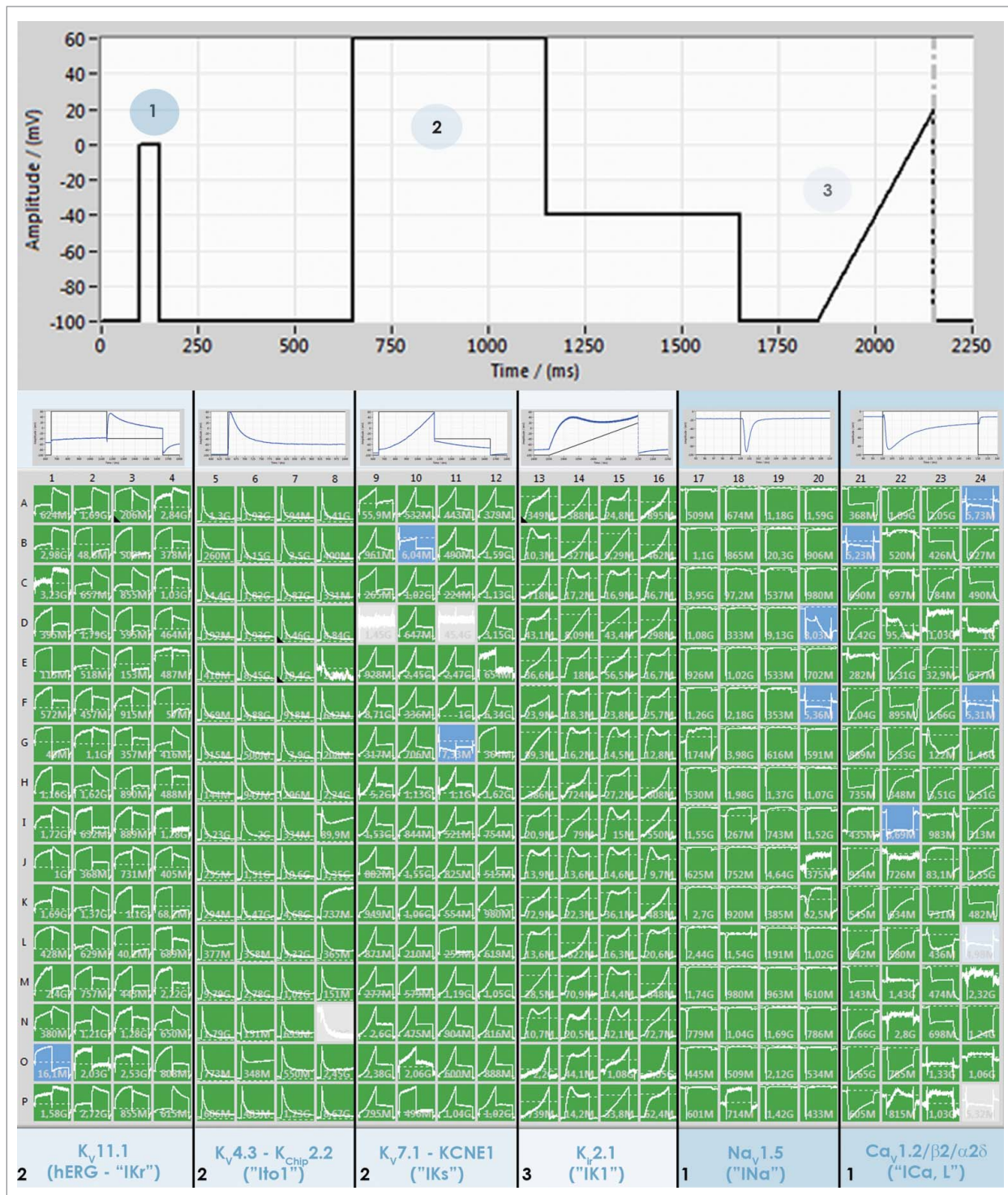


**Figure 3.** Screenshot of PatchControl 384, the software for the SyncroPatch 384PE, during a recording of 6 cardiac ion channels expressed in different cell lines. Four columns of the patch clamp chip (64 wells) received one cell line expressing either hERG (HEK),  $K_v4.3$  (CHO),  $K_v7.1$  (CHO), Kir2.1 (HEK),  $Na_v1.5$  (CHO) or  $Ca_v1.2$  (CHO). All cell lines were provided by ChanTest (a Charles River Company). A voltage protocol was designed to activate all channels simultaneously, shown at the top of the figure. The first step to 0 mV (1) was used to activate  $Na_v1.5$  and  $Ca_v1.2$ , the second part of the protocol to 60 mV followed by a step to -40 mV (2) was used to activate  $K_v4.3$ , hERG and  $K_v7.1$  and the final ramp (3) was used to activate Kir2.1. The columns are scaled individually to expand the relevant current and an example is shown at the top of each set of columns.

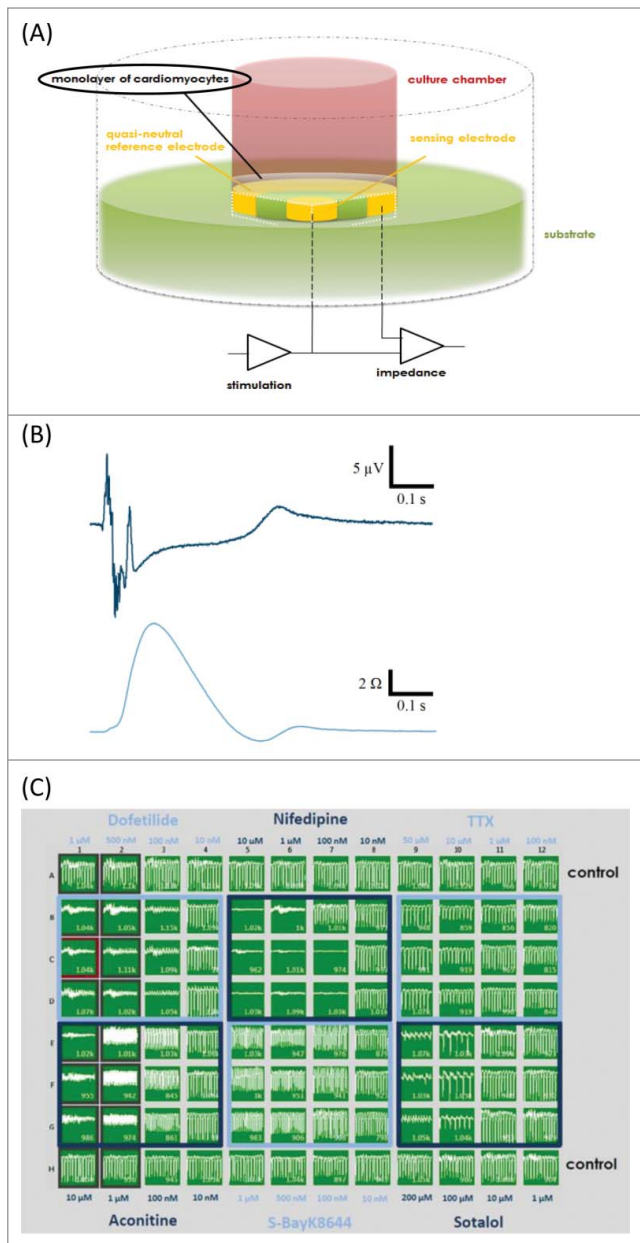


**Figure 4.** (A) Schematic setup of impedance measurement electrodes in the CardioExcyte 96 (Nanon Technologies). (B) The CE96 is capable of performing impedance and EFP recordings in combination. Top trace shows an EFP recording which represents the electrophysiological activity, the bottom trace shows the corresponding impedance trace which represents the contractility of the beating network. Note that the spikes in the beginning of the EFP trace are due to the fact that one recording electrode is used with which the electrical activity of the complete cardiomyocyte network is detected, translocation of the signal thus results in slightly shifted Na spikes. (C) 96-well view of an exemplary experimental layout in the impedance mode. Different concentrations of compounds were tested on Cor.4U cardiomyocytes (Axiogenesis). The compound-induced effects on the beat rate, amplitude or beat irregularity (arrhythmia), among other parameters, can be viewed online during the experiment. Panels (A and C) reproduced with permission from Doerr et al.<sup>32</sup> © SAGE. Reproduced by permission of Michelle Binur. Permission to reuse must be obtained from the rightsholder.

function in different cell preparations. When automated patch clamp systems are used, this is typically performed on individual cells that have been isolated. To address the next, more complex, hierarchical level of tissue organization, electrophysiological impedance measurements and multi-electrode arrays have proven particularly useful. These techniques allow cells to be studied within their physiological network of cells.

The xCELLigence RTCA Cardio-96 (ACEA Biosciences and Roche Applied Sciences) and the CardioExcyte 96 (Nanon Technologies) are commercially available systems that have been applied successfully to cardiomyocytes and stem cell-derived cardiomyocytes. Measurements are performed by non-invasive read-out of impedance and extracellular field potentials (EFP) for continuously monitoring beating myocytes that are placed in specifically designed wells including the measurement microelectrodes (Fig. 4A). Both systems operate using a 96-well format. A low alternating voltage signal (less than 20 mV) can be applied to the microelectrodes at the bottom of each well, to generate an oscillating electric field. The substantial mechanical modulation of cell morphology and adhesion that accompanies cardiomyocyte contraction is then monitored in the impedance signal, which in turn provides a dynamic and continuous readout of cardiac cell function. The EFP signal is passively recorded by differential voltage recordings (one recording, one reference electrode; Fig. 4A). The systems can be placed in a tissue culture incubator to provide the cells with an atmosphere that facilitates long-term (several days) of measurement time to study both short- and long-term effects of compounds on cardiomyocyte function. The CardioExcyte 96 can be alternatively used in combination with a climate chamber which controls temperature, humidity and gas mix similar to that of an incubator. The xCELLigence System acquires data at 12.9 ms,<sup>31</sup> while the CardioExcyte 96 allows sampling down to 1 ms data acquisition for the entire 96-well plate.<sup>32</sup> Both systems are capable of cardiac pacing in the impedance mode, controlling the beat rate of the cardiomyocytes by applying electrical stimuli.

With directly providing readout for the mechanical beating of cardiomyocytes, the label-free impedance technology has the potential to bridge the gap between direct cardiac ion channel patch clamp measurements on the one hand, and animal models on the other. This is especially relevant for cardiac safety assessments that are an important part of the drug discovery and development process. Impedance measurements have been validated for mouse embryonic stem cell-derived cardiomyocytes,<sup>32</sup> human iPS cardiomyocytes,<sup>32</sup> rat neonatal primary cardiomyocytes<sup>31,33</sup> and further cell lines, e.g. cardiac muscle cells (HL-1) and 3D cell clusters (hES-CMC<sup>TM</sup>).<sup>32</sup> It has been recognized that, while the interpretation of impedance data from cardiac cells is complex, these have the potential to provide relevant information on compound action, particularly for compounds that have more than one isolated ion channel effect. The schematic setup of impedance measurement electrodes in the CardioExcyte 96 is displayed in Figure 4A. Figure 4B shows an EFP trace and the corresponding impedance trace representing the contraction. Figure 4C shows a screenshot of the data acquisition software for the

CardioExcyte 96 during an experiment. Shown is the impedance view after application of 6 different compounds (plus control).

Interestingly, impedance measurements have been shown to be applicable to cells beyond cardiomyocytes. Recently, the technique has been applied to setting up an assay for determining virucidal activity of a chemical disinfectant, negating the necessity for subjective visual interpretation of light microscopy images of established protocols.<sup>34</sup> Also, proliferation of PC12 cells has been monitored by impedance technology to establish an assay for high-throughput screening of compounds for drugs against Alzheimer disease.<sup>35</sup> In this assay, amyloid- $\beta$  peptide A $\beta$ 1–42-induced apoptosis in PC12 cells is assessed by monitoring the proliferation and motility of the cells in real time. Adding to the growing numbers of assays set up with impedance measurements, brain endothelial cells have been immunologically analyzed and profiled with respect to their differential regulation by the pro-inflammatory regulators TNF $\alpha$  and IL-1 $\beta$ , employing xCELLigence biosensor technology.<sup>36</sup>

Multi-Electrode Arrays (MEA) are designed by embedding a larger number of electrodes in the bottom of a well in which cells are placed. In this way, more detailed information, especially at a high spatial resolution, on complex physiological networks can be unravelled. In the well of an in-vitro MEA, typically 8  $\times$  8 or

6  $\times$  10, electrodes are integrated, but custom designs with up to 256 electrodes have been reported. Besides the analysis of cardiac cells,<sup>37</sup> MEAs have proven particularly useful for the analysis of neuronal preparations, and stimulation parameters for dissociated cultures using MEAs have been published.<sup>38</sup> In a recent example, 2 organotypic spinal cord slices have been placed adjacently on multi-electrode arrays, and functional regeneration of intraspinal connections was shown by observing the synchronization of spontaneously occurring bursts in neuronal activity.<sup>39</sup> Also, 3-dimensional MEAs have been designed, and spikes corresponding to single cell activity in the hippocampal CA3 and CA1 regions in acute brain slices using such electrodes have been identified.<sup>40</sup> In a recent excellent review by Spira and Hai,<sup>41</sup> current MEA uses for studying neuronal circuit-connectivity and physiology and novel approaches combining extracellular arrays and intracellular microelectrodes are described.

#### Disclosure of Potential Conflicts of Interest

AO, SSF, NB, AB and NF are employees of Nanion Technologies, a manufacturer of Automated Patch Clamp instrumentation.

#### References

- Kaczorowski GJ, McManus OB, Priest BT, Garcia ML. Ion channels as drug targets: the next GPCRs. *J Gen Physiol* 2008; 131:399–405; PMID:18411331; <http://dx.doi.org/10.1085/jgp.200709946>
- Cavero I, Holzgreffe H. CiPA: Ongoing testing, future qualification procedures, and pending issues. *J Pharmacol Toxicol Methods* 2015; 76:27–37; PMID: 26159293; <http://dx.doi.org/10.1016/j.vascn.2015.06.004>
- Möller C, Slack M. Impact of new technologies for cellular screening along the drug value chain. *Drug Discov Today* 2010; 15:384–90; <http://dx.doi.org/10.1016/j.drudis.2010.02.010>
- Neher E, Sakmann B. Single-channel currents recorded from membrane of denervated frog muscle fibres. *Nature* 1976; 260:799–802
- Fertig N, Blick RH, Behrends JC. Whole cell patch clamp recording performed on a planar glass chip. *Biophys J* 2002; 82:3056–62; [http://dx.doi.org/10.1016/S0006-3495\(02\)75646-4](http://dx.doi.org/10.1016/S0006-3495(02)75646-4)
- Bébarová M. Advances in patch clamp technique: towards higher quality and quantity. *Gen Physiol Biophys* 2012; 31:131–40; PMID:22781816; [http://dx.doi.org/10.4149/gpb\\_2012\\_016](http://dx.doi.org/10.4149/gpb_2012_016)
- Dunlop J, Bowlby M, Peri R, Vasilyev D, Arias R. High-throughput electrophysiology: an emerging paradigm for ion-channel screening and physiology. *Nat Rev Drug Discov* 2008; 7:358–68; <http://dx.doi.org/10.1038/nrd2552>
- Farre C, Haythornthwaite A, Haarmann C, Stoelzle S, Kreir M, George M, Brüggemann A, Fertig N. Port-a-patch and patchliner: high fidelity electrophysiology for secondary screening and safety pharmacology. *Comb Chem High Throughput Screen* 2009; 12:24–37; PMID:19149489
- Mergler S, Garreis F, Sahlmüller M, Reinach PS, Paulsen F, Pleyer U. Thermosensitive transient receptor potential channels in human corneal epithelial cells. *J Cell Physiol* 2011; 226:1828–42; PMID:21506114; <http://dx.doi.org/10.1002/jcp.22514>
- Stoelzle S, Haythornthwaite A, Kettenhofen R, Kossolov E, Bohlen H, George M, Brüggemann A, Fertig N. Automated patch clamp on mESC-derived cardiomyocytes for cardiotoxicity prediction. *J Biomol Screen* 2011; 16:910–16; PMID:21775699; <http://dx.doi.org/10.1177/1087057111413924>
- Schieder M, Rötzer K, Brüggemann A, Biel M, Wahl-Schott C. Planar patch clamp approach to characterize ionic currents from intact lysosomes. *Sci Signal* 2010; 3:pl3; PMID:21139138; <http://dx.doi.org/10.1126/scisignal.3151pl3>
- Shaya D, Kreir M, Robbins RA, Wong S, Hammon J, Brüggemann A, Minor DL. Voltage-gated sodium channel (Nav) protein dissection creates a set of functional pore-only proteins. *Proc Natl Acad Sci USA* 2011; 108:12313–18; PMID:21746903; <http://dx.doi.org/10.1073/pnas.1106811108>
- Mahendran KR, Kreir M, Weingart H, Fertig N, Winterhalter M. Permeation of antibiotics through *Escherichia coli* OmpF and OmpC porins: screening for influx on a single-molecule level. *J Biomol Screen* 2010; 15:302–07; PMID:20086208; <http://dx.doi.org/10.1177/1087057109357791>
- Stoelzle S, Obergrussberger A, Brüggemann A, Haarmann C, George M, Kettenhofen R, Fertig N. State-of-the-Art Automated Patch Clamp Devices: Heat Activation, Action Potentials, and High Throughput in Ion Channel Screening. *Front Pharmacol* 2011; 2:76; PMID:22131976; <http://dx.doi.org/10.3389/fphar.2011.00076>
- Milligan CJ, Möller C. Automated planar patch-clamp. *Methods Mol Biol* 2013; 998:171–87; PMID:23529429; [http://dx.doi.org/10.1007/978-1-62703-351-0\\_13](http://dx.doi.org/10.1007/978-1-62703-351-0_13)
- Hao Y, Tang J, Wang K. Development of Automated Patch Clamp Assay for Evaluation of  $\alpha 7$  Nicotinic Acetylcholine Receptor Agonists in Automated QPatch-16. *Assay Drug Dev Technol* 2015; 13:174–84; PMID:25880723; <http://dx.doi.org/10.1089/adt.2014.622>
- Obergrussberger A, Haarmann C, Rinke I, Becker N, Guinot D, Brüggemann A, Stoelzle-Feix S, George M, Fertig N. Automated Patch Clamp Analysis of nACh $\alpha 7$  and Nav 1.7 Channels. *Curr Protoc Pharmacol* 2014; 65:11.13.1–11.13.48; PMID:24934604; <http://dx.doi.org/10.1002/0471141755.ph1113s65>
- Kauthale RR, Dadarkar SS, Husain R, Karande VV, Gatne MM. Assessment of temperature-induced HERG channel blockade variation by drugs. *J Appl Toxicol* 2015; 35:799–805; PMID:25348819; <http://dx.doi.org/10.1002/jat.3074>
- Papakosta M, Dalle C, Haythornthwaite A, Cao L, Stevens EB, Burgess G, Russell R, Cox PJ, Phillips SC, Grimm C. The chimeric approach reveals that differences in the TRPV1 pore domain determine species-specific sensitivity to block of heat activation. *J Biol Chem* 2011; 286:39663–72; PMID:21911503; <http://dx.doi.org/10.1074/jbc.M111.273581>
- Milligan CJ, Li J, Sukumar P, Majeed Y, Dallas ML, English A, Emery P, Porter KE, Smith AM, McFadzean I, et al. Robotic multiwell planar patch-clamp for native and primary mammalian cells. *Nat Protoc* 2009; 4:244–55; PMID:19197268; <http://dx.doi.org/10.1038/nprot.2008.230>
- Minetti G, Egée S, Mörsdorf D, Steffen P, Makhro A, Achilli C, Ciana A, Wang J, Bouyer G, Bernhardt I, et al. Red cell investigations: art and artefacts. *Blood Rev* 2013; 27:91–101; PMID:23425684; <http://dx.doi.org/10.1016/j.blre.2013.02.002>
- Li J, Sukumar P, Milligan CJ, Kumar B, Ma Z, Munsch CM, Jiang L, Porter KE, Beech DJ. Interactions, functions, and independence of plasma membrane STIM1 and TRPC1 in vascular smooth muscle cells. *Circ Res* 2008; 103:e97–104; PMID:18802022; <http://dx.doi.org/10.1161/CIRCRESAHA.108.182931>
- Kettenhofen R, Bohlen H. Preclinical assessment of cardiac toxicity. *Drug Discov Today* 2008; 13:702–07; <http://dx.doi.org/10.1016/j.drudis.2008.06.011>
- Möller C, Witchel H. Automated electrophysiology makes the pace for cardiac ion channel safety screening. *Front Pharmacol* 2011; 2:73; PMID:22131974; <http://dx.doi.org/10.3389/fphar.2011.00073>
- Pierson JB, Berridge BR, Brooks MB, Dreher K, Koerner J, Schultze AE, Sarazan RD, Valentin J, Vargas HM, Pettit SD. A public-private consortium advances cardiac safety evaluation: achievements of the HESI Cardiac Safety Technical Committee. *J Pharmacol Toxicol Methods* 2013; 68:7–12; PMID:23567075; <http://dx.doi.org/10.1016/j.vascn.2013.03.008>
- Becker N, Stoelzle S, Göpel S, Guinot D, Mumm P, Haarmann C, Malan D, Bohlen H, Kossolov E, Kettenhofen R, et al. Minimized cell usage for stem



- cell-derived and primary cells on an automated patch clamp system. *J Pharmacol Toxicol Methods* 2013; 68:82-87; PMID:23567076; <http://dx.doi.org/10.1016/j.vascn.2013.03.009>
27. Okada J, Yoshinaga T, Kurokawa J, Washio T, Furukawa T, Sawada K, Sugiura S, Hisada T. Screening system for drug-induced arrhythmogenic risk combining a patch clamp and heart simulator. *Science Advances* 2015; 1:e1400142-e1400142; <http://dx.doi.org/10.1126/sciadv.1400142>
  28. Haythornthwaite A, Stoelzle S, Hasler A, Kiss A, Mosbacher J, George M, Brüggemann A, Fertig N. Characterizing human ion channels in induced pluripotent stem cell-derived neurons. *J Biomol Screen* 2012; 17:1264-72; PMID:22923790; <http://dx.doi.org/10.1177/1087057112457821>
  29. Slack M, Kirchhoff C, Moller C, Winkler D, Netzer R. Identification of novel Kv1.3 blockers using a fluorescent cell-based ion channel assay. *J Biomol Screen* 2006; 11:57-64; <http://dx.doi.org/10.1177/1087057105282712>
  30. Solly K, Klein R, Rudd M, Holloway MK, Johnson EN, Henze D, Finley MFA. High-Throughput Screen of GluK1 Receptor Identifies Selective Inhibitors with a Variety of Kinetic Profiles Using Fluorescence and Electrophysiology Assays. *J Biomol Screen* 2015; 20:708-19; PMID:25700884; <http://dx.doi.org/10.1177/1087057115570580>
  31. Xi B, Wang T, Li N, Ouyang W, Zhang W, Wu J, Xu X, Wang X, Abassi YA. Functional cardiotoxicity profiling and screening using the xCELLigence RTCA Cardio System. *J Lab Autom* 2011; 16:415-21; PMID:22093298; <http://dx.doi.org/10.1016/j.jala.2011.09.002>
  32. Doerr L, Thomas U, Guinot DR, Bot CT, Stoelzle-Feix S, Beckler M, George M, Fertig N. New easy-to-use hybrid system for extracellular potential and impedance recordings. *J Lab Autom* 2015; 20:175-88; PMID:25532527; <http://dx.doi.org/10.1177/2211068214562832>
  33. Abassi YA, Xi B, Li N, Ouyang W, Seiler A, Watzele M, Kettenhofen R, Bohlen H, Ehlich A, Kolosov E, et al. Dynamic monitoring of beating periodicity of stem cell-derived cardiomyocytes as a predictive tool for preclinical safety assessment. *Br J Pharmacol* 2012; 165:1424-41; PMID:21838757; <http://dx.doi.org/10.1111/j.1476-5381.2011.01623.x>
  34. Ebersohn K, Coetzee P, Venter EH. An improved method for determining virucidal efficacy of a chemical disinfectant using an electrical impedance assay. *J Virol Methods* 2014; 199:25-8; PMID:24389126; <http://dx.doi.org/10.1016/j.jviromet.2013.12.023>
  35. Hou X, Yan R, Yang C, Zhang L, Su R, Liu S, Zhang S, He W, Fang S, Cheng S, et al. A novel assay for high-throughput screening of anti-Alzheimer's disease drugs to determine their efficacy by real-time monitoring of changes in PC12 cell proliferation. *Int J Mol Med* 2013; 33(3):543-9; PMID:24378397; <http://dx.doi.org/10.3892/ijmm.2013.1608>
  36. O'Carroll SJ, Kho DT, Wiltshire R, Nelson V, Rotimi O, Johnson R, Angel CE, Graham ES. Pro-inflammatory TNF $\alpha$  and IL-1 $\beta$  differentially regulate the inflammatory phenotype of brain microvascular endothelial cells. *J Neuroinflammation* 2015; 12:131; PMID:26152369; <http://dx.doi.org/10.1186/s12974-015-0346-0>
  37. Uesugi M, Ojima A, Taniguchi T, Miyamoto N, Sawada K. Low-density plating is sufficient to induce cardiac hypertrophy and electrical remodeling in highly purified human iPS cell-derived cardiomyocytes. *J Pharmacol Toxicol Methods* 2013; 69(2):177-88; PMID:24296355; <http://dx.doi.org/10.1016/j.vascn.2013.11.002>
  38. Wagenaar DA, Pine J, Potter SM. Effective parameters for stimulation of dissociated cultures using multi-electrode arrays. *J Neurosci. Methods* 2004; 138:27-37; PMID:15325108; <http://dx.doi.org/10.1016/j.jneumeth.2004.03.005>
  39. Heidemann M, Streit J, Tschertner A. Functional regeneration of intraspinal connections in a new in vitro model. *Neuroscience* 2014; 262:40-52; PMID:24394955; <http://dx.doi.org/10.1016/j.neuroscience.2013.12.051>
  40. Heuschkel MO, Fejt M, Raggenbass M, Bertrand D, Renaud P. A three-dimensional multi-electrode array for multi-site stimulation and recording in acute brain slices. *J Neurosci Methods* 2002; 114:135-48; PMID:11856564
  41. Spira ME, Hai A. Multi-electrode array technologies for neuroscience and cardiology. *Nat Nanotechnol* 2013; 8:83-94; PMID:23380931; <http://dx.doi.org/10.1038/nnano.2012.265>
  42. Brüggemann A, Stoelzle S, George M, Behrends JC, Fertig N. Microchip technology for automated and parallel patch-clamp recording. *Small* 2006; 2:840-46; PMID:17193131; <http://dx.doi.org/10.1002/sml.200600083>